

Interference Drag Between Spherical and Cylindrical Particles in Stokes Flow

A.K.W. Cheung, B.T. Tan, K. Hourigan, M.C. Thompson

Fluids Laboratory for Aeronautical and Industrial Research (FLAIR)
Department of Mechanical Engineering
Monash University, Victoria, 3800 AUSTRALIA

Abstract

In this study, predictions are made for the interference effects when two cylinders or two spheres are placed in series or parallel in a low Reynolds number flow. Using a spectral element method, it is predicted that for two cylinders with their line of centres perpendicular to the flow, the drag force is lower than the isolated cylinder case at small gaps but is greater at all other gaps; a maximum is found at a gap of approximately of 7 cylinder diameters. The result is fundamentally different to the case of two spheres with their line of centres perpendicular to the flow, which has an analytical value reported in Happel and Brenner [7]; in that case the drag force on each sphere is less than an isolated sphere at all gaps. For cylinders with their lines of centres parallel to the flow, the drag on the trailing body is less than the leading body, which in turn is less than the drag on an isolated cylinder. In the case of spheres, the drag on the individual bodies is similar and less than the drag on an isolated body for all gaps. However, in the case of cylinders, the drag on the leading body is significantly greater than that on the trailing cylinder.

Introduction

There have been great advances in the measurement, prediction and understanding of the flows around bluff bodies over the past decade. This has been stimulated by the widespread presence of bluff bodies in most areas of fluid flows - liquid-solid flows, planetary aggregation, sporting ball flight, and even aircraft which have bluff components, such as nacelles and the fuselage in cross-wind. At the industrial level, liquid such as water is employed to transport particles in the mining, mineral processing, manufacturing and waste disposal industries. The efficiency of transport and the attendant problems of fouling, deposition and wear, are all influenced by the collisions that occur at the micro level; that is, the effect of the collisions and interactions between the particles. The development of Digital Particle Image Velocimetry (DPIV) is allowing the instantaneous capture of entire regions of fluid flows; the further development of Holographic DPIV will enable the capture of full three-dimensional fields. Advances in high-order techniques such as the spectral element method and its implementation on high speed parallel machines is resulting in the accurate prediction of relatively fine scale structures for low Reynolds number flows. The richness of the wakes of bluff body flows at moderate Reynolds numbers has been enhanced by the relatively recent discoveries of the different instability modes, A and B, and possibly S.

Liquid-solid flows occur in many industrial processes. The behaviour of the flow and the motions of the particles in these fluids are dependent on the outcomes of the many interactions that occur continually between particles and bounding walls. In dry granular flows (negligible interstitial fluid), the coefficient of restitution (defined by the ratio of the rebound to impact velocity) characterises the amount of energy dissipation due to

the inelasticity of the particle contacts. Likewise, in liquid-solid flows where the interstitial fluid is important, the effective coefficient of restitution is important in describing collisions. In this case, it is required to take into account the viscous dissipation and kinetic energy needed to displace the fluid between the surfaces in addition to the inelasticity of the contact. In recent numerical simulations of liquid-solid flows (Hu [9], Glowinski [6]), although the motion of the interstitial fluid is calculated directly, the interaction between particles is modelled in a limited fashion through a repulsive force between the particles, which prevents particles actually contacting.

The basic problem of a sphere moving towards a surface or toward another sphere in a fluid has been the subject of many studies. Earlier studies (Brenner [3]; Davis *et al.* [4]) led to the identification of the particle Stokes number and an elasticity parameter as important parameters of the collision process. The Stokes number is defined as $St = mv_0/(6\pi\mu a^2) = (1/9)Re(\rho_p/\rho_f)$ and the elasticity parameter $\epsilon = 4\theta\mu v_0 a^{3/2}/x_0^{5/2}$, where θ depends on the Young's modulus and Poisson's ratio of the two bodies; x_0 is the position within the gap between the undeformed surfaces at which the velocity is v_0 , and $a = d/2$ is the particle radius. Their analyses assume that the Reynolds number Re is much less than unit, giving results independent of fluid density.

Later studies by Barnocky and Davis [1] included the variation of density and viscosity with pressure; it was observed that an increase in density of the fluid during compression could enhance the rebound of an impacting particle, even when the particle was completely rigid. A perturbation study along similar lines was carried out by Kytomaa and Schmid [10]; it was conjectured that a non-linear dependence on pressure might result in a rebound of even incompressible particles.

The lubrication layer between two colliding particles can be of the same order as the surface roughness, as pointed out by Smart and Leighton [16]. Measurements of the coefficient of restitution when a drop of fluid was placed in the gap between a sphere impacting on a surface were undertaken by Lundberg and Shen [13] and Barnocky and Davis [1]; the latter showed that a critical Stokes number was present and above which rebound occurs. Some experimental studies have examined the rebound of a particle falling at its terminal velocity and impacting a submerged surface (McLaughlin [14]; Gondret *et al.* [7]). Particles were dropped into a tank immersed in various viscous fluids to study the transition from arrest to rebound. Over a range of Reynolds numbers, there was a critical Stokes number (typically around 10) below which rebound did not occur.

Recent experiments undertaken at Caltech (Zenit and Hunt, [20]; Joseph *et al.* [11]) have shown that the elastic properties of the particles and the walls do not have a significant effect on the measured coefficients of restitution. For a particle colliding with a wall in the normal direction, a deceleration was observed due to

the presence of the wall at Stokes numbers lower than approximately 70, with rebound ceasing at approximately 10. The distance from the wall at which the particle commences to decelerate increases with decreasing Stokes number. For Stokes numbers above 70, there is no apparent deceleration and above about 2000, the fluid effects can be neglected.

Low Reynolds number flow around objects in proximity has been the subject of research for many years. A mathematical model was constructed by Stimson and Jeffery [17]. The solution was based on determining the Stokes stream function of the motion of the fluid:

$$F_z = \mu\pi \int \rho^3 \frac{\partial}{\partial n} \left(\frac{E^2 \psi}{\rho^2} \right) ds \quad (1)$$

where n is the normal drawn outward from the solid and ρ is the distance from the axis. The integral is taken around the meridian section of the solid making a positive right angle with the direction n .

Happel and Brenner [7] simplified this further to:

$$F_z = 6\pi\mu a U \lambda \quad (2)$$

where a is the radius of either sphere and λ can be defined as a ratio of the drag of one of the spheres to the drag of a sphere in an unbounded fluid [15].

Experiments were also performed by Happel and Brenner [7] to investigate the change of drag ratio with varying distance between two spheres, both in a flow parallel and perpendicular to the line of centres. However, details of the experiment setup were not disclosed.

Lecoq *et al.* [12] had an experimental investigation of the hydrodynamic interactions between a sphere and a large spherical obstacle. The experiment involved dropping a steel ball immersed in a viscous fluid towards the spherical object with the aid of gravity. The velocity data of the steel ball was recorded using a series of mirrors and laser beam arrangement [12].

Using CFD to investigate the interaction between two spheres in fluid flow has been rare. In this paper, a spectral element method is used to investigate the change of drag of the spheres and cylinders in fluid flow with respect to the change of distance between them. This study represents the first stage of a project that will use direct numerical simulation of particle-particle and particle-wall collisions over a range of Reynolds numbers in ensemble and near walls. The aim is to test the numerical code on interference between fixed particles in flows, both in parallel and in series or tandem, at low Reynolds numbers and compare with previous experimental results.

Approach

Numerical prediction method

The spectral element code was developed at Monash and has been successfully used by Thompson *et al.* [18, 19] in the first prediction the wavelengths of both wake modes, A and B, in the wake of a circular cylinder. The spectral-element method is a higher-order finite-element approach. For each element the node points lie at the quadrature points of a particular Gauss quadrature formula. In this case, the nodes correspond to Gauss-Lobatto points and Gauss-Legendre-Lobatto quadrature is used to approximate the integrations over elements resulting from the application of the Galerkin finite element method to the Navier-Stokes equations.

Accuracy of the code is tested by calculating the drag of a single cylinder in a flow with Reynolds number equals to 1. From Fox and MacDonald [5], it can be seen that the drag coefficient is approximately 12.42. Using the spectral element code, the calculated drag computed is equalled to 12.32 which is within 1% of the experimental result.

Cases

The cases being investigated involve the drag ratio change of two cylinders with the flow parallel and perpendicular to their line of centres with respect to increasing distance between them. The drag ratio is defined as the drag of a cylinder over the drag of a cylinder in an infinite medium. The distance (edge to edge), l between the cylinders is converted to a non-dimensional variable by dividing the distance by the diameter of the cylinder, $l/2r_0$.

This paper will also look at the effect of drag ratio change between two spheres in a flow parallel to their line of centres with respect to increasing the distance in between. The result will be compared to those of Happel and Brenner's [7] for accuracy.

The Grid - Cylinders

The grid for each case was generated using the commercial software Gambit. Each file was saved as a suitable format to be compatible with Spectral Element Code. A typical grid for the flow around two cylinders is shown in figure 1 below.

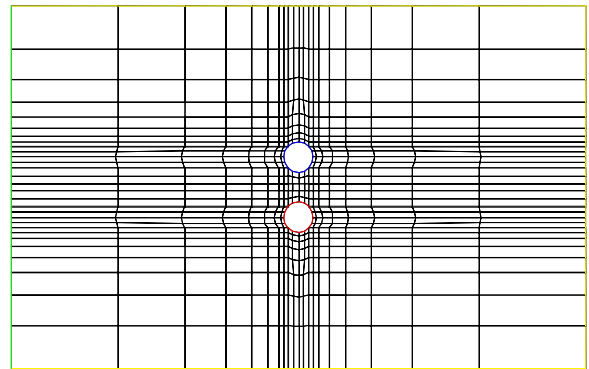


Fig. 1. Macroelements of the numerical mesh for the case of two cylinders with flow perpendicular to the line of centres. The distance between them is $l/2r_0 = 1$

The diameters of the two cylinders are taken to be identical. The vertical margin between the cylinders and the slip wall (the top and bottom edge) is fifty cylinder diameters, while the horizontal margin is set at twenty cylinder diameters. Flow was introduced from left to right and the Reynolds number was set to unity.

The Grid – spheres

The flow around two spheres was run assuming axisymmetry, which is appropriate due to the low Reynolds number. A typical axisymmetric numerical grid for the two-sphere case is shown in figure 2.

The diameters of the two spheres are identical; the margins were set identical to those of the cylinders' cases. The Reynolds number, based on sphere diameter and upstream flow was set at 0.05, for comparison with previous experimental results.

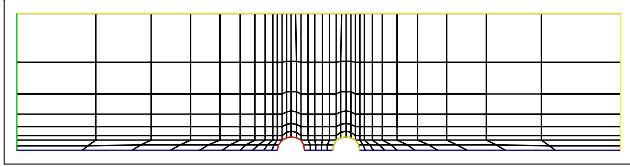


Fig. 2. Macroelements of the numerical mesh for the case of two spheres with flow parallel to their line of centres.

Results and Discussion

Flow around Cylinders - Flow perpendicular to line of centres

The contours of vorticity are shown in Fig. 3 for the isolated cylinder and for different gaps, $l/2r_0$, between two cylinders for flow at a Reynolds number of unity. The viscous interference effect is clear even when the cylinders are far apart. The drag on each cylinder relative to the isolated cylinder case is plotted for different gaps in Fig. 4. It is interesting to note that the relative drag exceeds unity when the gap is greater than approximately 3, reaches a maximum at about a gap of 7 and then asymptotes slowly towards unity as the gap is increased. This is similar to a particle falling in a fluid close to a wall where the wall has a retarding effect [15], causing an increase in drag.

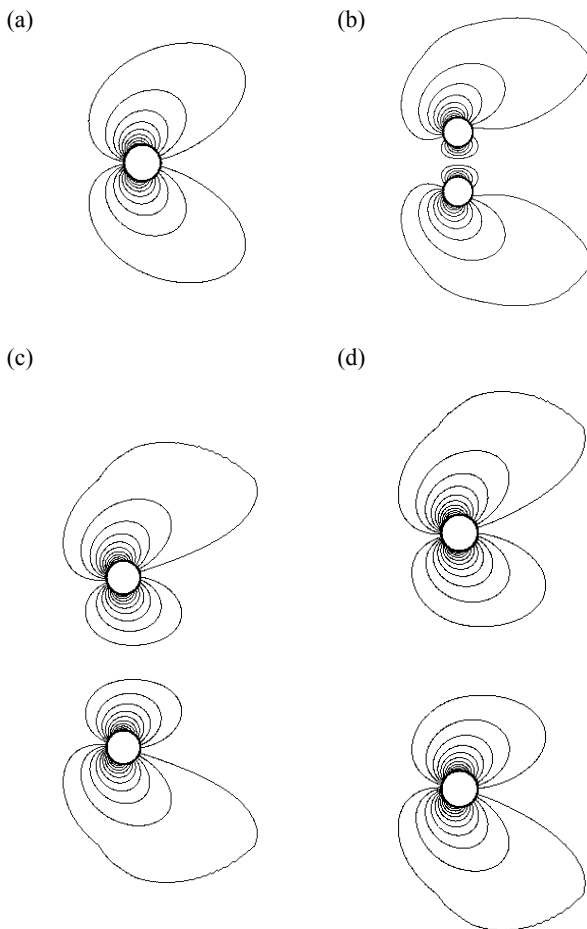


Fig. 3. Plots of streamlines for different cylinder gaps (flow from left to right) (a) $l/2r_0 = 0$, (b) $l/2r_0 = 1.0$, (c) $l/2r_0 = 4.0$, (d) $l/2r_0 = 6.0$.

It is interesting to consider the total force coefficient on the cylinders. This is shown in Fig. 5, with the arrow directions indicating the component of lift compared with the drag. Whereas for small gaps the drag ratio is less than unity (see Fig. 4), the total force on the body is greater than for the isolated case

for all gaps. The theoretical value of the drag coefficient for a circular cylinder is given in [2] as $C_D = 8\pi/[Re \log(7.4/Re)] \approx 12.56$ for $Re = 1$, which is close to the predicted value of 12..32.

Flow around Cylinders - Flow parallel to line of centres

In this case, the wake of the leading cylinder exerts a strong influence on the trailing cylinder, as shown in Fig. 6. Both cylinders experience a lower drag as the gap decreases; due to the symmetry, no lift forces are found. Note however that the drag on the trailing cylinder is significantly lower than that on the leading cylinder. This is akin to the phenomenon of ‘slip-streaming’ observed at much higher Reynolds numbers in motor racing where a car following closely behind another car would experience a reduction in drag.

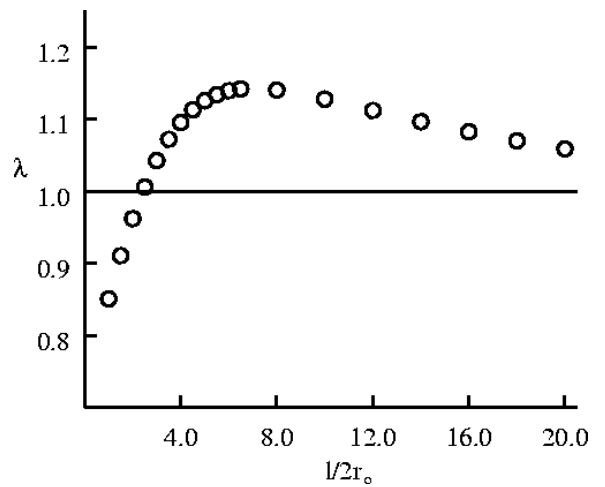


Fig.4. Plot of drag ratio vs spacing for two cylinders in a flow perpendicular to the line of centres

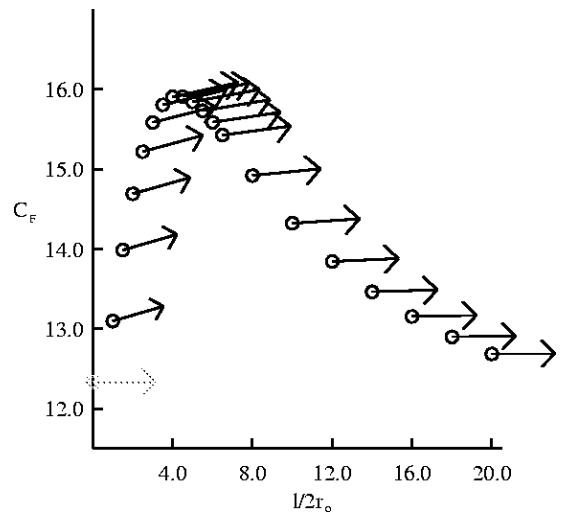


Fig. 5. Plot of total force on the upper of the two cylinders for cylinders with flow perpendicular to the line of centres. Arrow shows direction, lower grey case is for single cylinder

Flow around Spheres in Series

Figure 6 shows how the drag ratio varies with respect to the distance between two spheres with their line of centres parallel to the flow at Reynolds number 0.05. In this case, the plots show a trend similar to that predicted by Happel and Brenner [7]. Distinct from the two cylinders case, the spheres possess near identical levels of drag. Evidently the flow recovers more rapidly

around a sphere at this low Reynolds number, as would be expected by their lower blockage. The predicted value, corrected for wall outer wall effects matches well the theoretical value of the drag on an isolated sphere is $C_D = 24/Re (1 + 3/16 Re)$ [2].

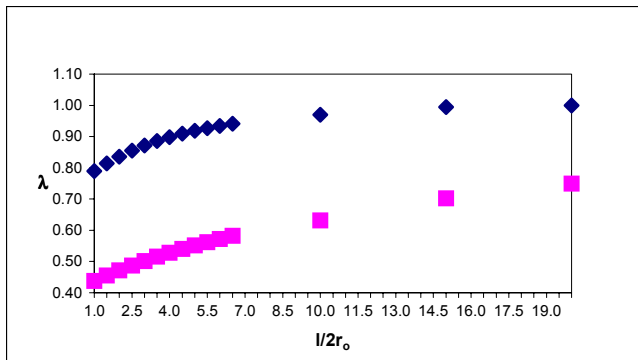


Fig. 6. Plot of drag ratio λ vs distance for two cylinders in a flow parallel to the line of centres. Leading cylinder (\diamond) and trailing cylinder (\square).

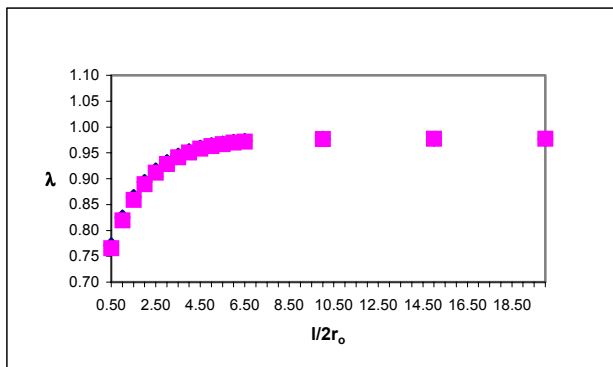


Fig. 7. Plot of drag ratio λ vs distance for two spheres in a flow parallel to the line of centres. Leading sphere (\diamond) and trailing sphere (\square).

Conclusions

In conclusion, it can be seen that the interference effect of two objects placed in proximity in a flow can be observed by the change of drag that the object experienced. Using a spectral element method, it has been predicted that for two cylinders with their line of centres perpendicular to the flow, the drag force is lower than the isolated cylinder case at small gaps but is greater at all other gaps; a maximum is found at a gap of approximately 7 cylinder diameters. This result is fundamentally different to the case of two spheres with their line of centres perpendicular to the flow, which has an analytical value reported in Happel and Brenner [7]; in that case the drag force on each sphere is less than an isolated sphere at all gaps.

When the lines of centres are parallel to the flow, in the case of spheres, the drag on each individual body is similar and less than the drag of an isolated body for all gaps. However, in the case of cylinders, the drag on the leading body is significantly greater than that on the trailing body; interference is evidently greater in the two-dimensional flow. For these low Reynolds number flows, the effect of the lateral boundaries at finite distances are greater and include reflections of the viscous field.

The next stage of the project will investigate the drag on a particle moving relative to another particle, or a wall, and rebound. Dynamic regridding will be employed to allow modelling of the relative motion and emphasis will be placed on the lubrication layer.

Acknowledgments

Alex Cheung would like to thank the Department of Mechanical Engineering at Monash University for the support of a Departmental Postgraduate Scholarship.

References

- [1] Barnocky, G. and Davis, R.H. 1989 The influence of pressure-dependent density and viscosity on the elasto-hydrodynamic collision and rebound of two spheres. *J. Fluid Mech.* **209**, 501-519.
- [2] Batchelor, G.K., *An Introduction to Fluid Dynamics*, Cambridge University Press, 1967.
- [3] Brenner, H. 1961 The slow motion of a sphere through a viscous fluid towards a plane surface. *Chem. Engng Sci.* **16**, 242-251.
- [4] Davis, R. H., Serayssol, J. M. & Hinch, E. J. 1986 The elasto-hydrodynamic collision of two spheres. *J. Fluid. Mech.* **163**, 479-497.
- [5] Fox, R.W. & McDonald, A.T., *Introduction to Fluid Mechanics*, New York, Wiley, 1994.
- [6] Glowinski, R., Pan, T., Hesla, T.I. and Joseph, D.D. 1999 A distributed Lagrange multiplier fictitious domain method for particulate flows. *Int. J. Multiphase Flow* **25** (5), 755-794.
- [7] Gondret, P., Hallouin, E., Lance, M. & Petit, L. 1999 Experiments on the motion of a solid sphere toward a wall: From viscous dissipation to elasto-hydrodynamic bouncing. *Phys. Fluids* **11** (9), 2803-2805.
- [8] Happel, J. & Brenner, H., *Low Reynolds Number Hydrodynamics*, Martinus Nijhoff, 1983.
- [9] Hu, H.H. 1996 Direct simulation of flows of solid-liquid mixtures. *Int. J. Multiphase Flow* **22** (2), 335-352
- [10] Kytomaa, H. & Schmid, P. 1992 On the collision of rigid spheres in a weakly compressible fluid. *Phys. Fluids A* **4** (12), 2683-2689.
- [11] Joseph, G.G., Zenit, R., Hunt, M.L. & Rosenwinkel, A.M. Particle-wall collisions in a viscous fluid, to appear *J. Fluid Mechanics* (2001).
- [12] Lecoq, N., Feuillebois, F., Anthor, R., Petipas, C. & Bostel, F., experimental investigation of the hydrodynamics interactions between a sphere and a large spherical obstacle, *J. Phys.*, **5**(2), Feb 1994, 323-334.
- [13] Lundberg, J. & Shen, H. 1992 Collisional restitution dependence on viscosity. *J. Eng. Mech.-ASCE* **118** (5), 979-989.
- [14] McLaughlin, M. H. 1968 An experimental study of particle-wall collision relating of flow of solid particles in a fluid. Engineer's degree thesis, California Institute of Technology, Pasadena, California.
- [15] Panton, R., *Incompressible Flow*, New York, Wiley, 1984.
- [16] Smart, J. R. & Leighton, D. T. 1989 Measurement of the hydrodynamic surface-roughness of noncolloidal spheres. *Phys. Fluids A* **1** (1), 52-60.
- [17] Stimson M. & Jeffrey G.B., Proc. Roy. Soc (London) A111 (1926), 110.
- [18] Thompson, M.C., Hourigan, K. & Sheridan, J. Three-dimensional instabilities in the wake of a circular cylinder. International Colloquium on Jets, Wakes and Shear Layers, 18-20 April, 1994 Melbourne, Australia.
- [19] Thompson, M.C, Hourigan, K. & Sheridan, J. Three-dimensional instabilities in the wake of a circular cylinder. *Exp. Thermal Fluid Sci.*, **12**, 1996, 190-196
- [20] Zenit, R. and Hunt, M.L. 1999 Mechanics of immersed particle collisions. *J. Fluid Eng.-T. ASME* **121** (1), 179-184.